Ceramics International xxx (xxxx) xxx–xxx

Contents lists available at ScienceDirect

Ceramics International

journal homepage: www.elsevier.com/locate/ceramint

Mechanical properties obtained by nanoindentation of sintered zircon–glass matrix composites

J.L. Amorós[a,b], E. Blasco[b,*], A. Moreno[a,b], C. Feliu[a,b]

[a] Department of Chemical Engineering, Universitat Jaume I, Campus Universitario Riu Sec, Castellón, 12006, Spain
[b] Instituto de Tecnología Cerámica, Asociación de Investigación de las Industrias Cerámicas, Castellón, 12006, Spain

ARTICLE INFO

Keywords:
Ceramic composites
Nanoindentation
Sintering

ABSTRACT

This study was undertaken to determine the effect of zircon content and firing temperature on the hardness and indentation modulus of zircon–glass composites obtained by sintering. A standard non-devitrified borosilicate glass (SRM 717a) powder and an industrial micrometric zircon powder were used to prepare mixtures with a zircon volume/solids volume between 0 and 0.63, by the wet method. The values of these mechanical properties were determined by nanoindentation and related to the most important microstructural characteristics of the composites, such as porosity, zircon volume fraction, glass volume fraction, and average zircon grain size. Composite mechanical performance was interpreted and determined by statistically analysing the results of a large number of indentations using two maximum loads. An empirical model was developed that describes the effect of these microstructural characteristics on composite hardness and modulus of indentation. Composites of high hardness (11.3 ± 2.5 GPa) and low porosity (ε = 0.07) were obtained at 1100 °C from a mixture with a zircon volume/solids volume of 0.43.

1. Introduction

Of the properties requiring only a small volume of material for their determination, the nanoindentation measurement of hardness best characterises a material's wear performance. This property is critical for glazed floor tiles. Many ceramic coatings, including ceramic glazes, consist of more or less complex glass matrix composites (GMCs). Zircon content has been shown to have a positive effect on glaze mechanical properties [1–6]. In no reported case, nor in industrial practice, however, does glaze zircon content exceed 12–15%, regardless of whether the zirconium is introduced as part of a frit or added as zircon. As a result, very little information is available on the effect of zircon on the mechanical properties of materials (glazes or GMCs) with a higher zircon content than that used in industry [7]. Similarly, only a few recent studies are available on the nanomechanical properties of glazes [8]. This study was therefore undertaken to examine the mechanical properties, by nanoindentation, of composites with a zircon content ranging from 0 to 0.63 zircon volume/solids volume, to establish a relationship between the microstructural characteristics of these materials and their nanomechanical properties. The resulting information is extremely useful when it comes to designing coatings, such as glazes for ceramic floorings intended for heavy traffic, which will be subjected to high abrasion.

In a previous study, sintered zircon–glass composites with different zircon volume/solids volume, $\phi \leq 0.63$, were obtained and microstructurally characterised. The results, mechanism, and kinetic model of the non-isothermal sintering process were described in previous papers [9,10]. This study was undertaken to determine the effect of the zircon content, ϕ, and firing temperature on the indentation modulus, M, and hardness, H, of these composites. These mechanical properties (M and H) were related to the most important microstructural characteristics of the composites, such as porosity, ε, zircon volume fraction, ϕ_z (zircon volume/total volume), glass volume fraction, ϕ_v (glass volume/total volume), and average zircon grain size, G. The effect of the maximum indentation load, P_{max}, on H and M was also determined. The mechanical performance of each composite was determined by statistically analysing the results of a large number of indentations.

2. Materials and methods

In a previous study, a standard non-devitrified borosilicate glass (SRM 717a) powder and an industrial micrometric zircon powder (Table 1) were used to prepare mixtures at different zircon volume/solids volume, ϕ, by the wet method. The microstructural characteristics of composites made up of these compositions were determined by scanning electron microscopy (SEM) (with EDS and image analysis) and

* Corresponding author.
E-mail address: encarna.blasco@itc.uji.es (E. Blasco).

https://doi.org/10.1016/j.ceramint.2020.01.075
Received 14 November 2019; Received in revised form 8 January 2020; Accepted 9 January 2020

Table 1
Values of d_{90}, d_{50}, and d_{10} for the glass and zircon powders, corresponding to less than 90%, 50%, and 10% by volume, respectively, of the particles.

Powder	d_{90} (μm)	d_{50} (μm)	d_{10} (μm)
Glass	17.7	5.6	1.5
Zircon	3.4	1.5	0.5

X-ray diffraction (XRD). The results have been published elsewhere [9,10].

In this study, cylindrical test pieces, about 2 × 2cm, obtained by slip casting from the above powders, were subjected to 5 K/min in a laboratory furnace. Each test composite surface to be mechanically tested was ground and diamond polished to a mirror-like surface finish following 9μm–1μm steps.

Nanoindentation measurements were performed using a Micromaterials Nanotest 600 indenter, with a Berkovich diamond tip, equipped with a continuous stiffness measurement module, which allowed dynamic determination of each material's properties during indentation from the load–displacement curves according to the Oliver and Pharr method [11,12]. Numerous nanoindentations (50 imprints in the case of the maximum applied load, P_{max} = 1 N, and 100 imprints for P_{max} = 100 mN) were performed with a distance between imprints of 50 μm. For P_{max} = 1 N, the loading rate was 100 mN/s; for P_{max} = 100 mN, this was10 mN/s. In both cases, dwell time at P_{max} was 10s.

The indentation data were analysed using some elementary statistics relations. It was assumed that the distribution of the property, X = M or H, of each mechanical component, j (glass, zircon grain, pore, and zircon–glass cluster), could be approximated by the normal or Gaussian distribution [13,14]:

$$p_j(X) = \frac{1}{\sqrt{2\pi\sigma_j^2}} exp\left(-\frac{(X-\bar{\mu}_j)^2}{2\sigma_j^2}\right) \quad (1)$$

where $\bar{\mu}_j$ is the arithmetic mean of all N_j values of each mechanical component and σ_j is its standard deviation. For P_{max} = 1 N, the bulk mechanical response of a large volume of material was obtained. In this case, the indentation results could be described by a single mechanical component. For P_{max} = 100 mN, deconvolution of the mechanical response distribution into four components was required to describe the experimental results. Thus, the probability distribution function was:

$$p(X) = \sum_{j=1}^{j=n} f_j p_j(X) \quad (2)$$

where f_j is the volume fraction of each mechanical component. In addition, the following shall be obeyed:

$$\sum_{j=1}^{j=n} f_j = 1 \quad (3)$$

3. Results and discussion

Nanoindentation allows determination of the H and M values of the representative volume element (RVE), whose characteristic size or length scale, L, is roughly $3h_{max}$ for Berkovich indentation [14]. For the composite with high zircon content, ϕ = 0.525, obtained at 1350 °C (Fig. 1), peak loading at P_{max} = 0.1 N led to an average maximum indentation depth, h_{max}, of ≈0.4 μm, which involved an RVE (solid triangles in Fig. 1b) with a length scale of L ≈ 1.2 μm, which was smaller than the following homogeneous areas shown in Fig. 1b: pores (referenced 1), glass matrix areas (referenced 2), clusters of small zircon grains embedded in the glass matrix (referenced 3), and large zircon grains (referenced 4). The overall H and M distribution was deconvoluted into four Gaussian distributions (eqs. (1) and (2)), each characterising its corresponding area (Fig. 1c). For P_{max} = 1 N, the average maximum indentation depth, h_{max}, was ≈2 μm; consequently, the RVE (empty yellow triangle) and L ≈ 6 μm were of the same order as or larger than the size of the areas of the four components mentioned above, so that a wide Gaussian distribution was obtained (Fig. 1a).

It was further confirmed that, for P_{max} = 0.1 N, on averaging the values of H (100 indentations), a larger arithmetic mean $\bar{H}$ = 12.6 GPa and standard deviation σ = 8.2 GPa were obtained than those found on using P_{max} = 1 N, $\bar{H}$ = 10.2 GPa, and σ = 2.7 GPa (Fig. 1a), owing to the so-called indentation size effect (ISE) [15,16]. It was also verified that, for P_{max} = 1 N, the average maximum indentation depth, h_{max}, was ≥1 μm, a critical value at which the ISE is negligible [15,16]. As a result, P_{max} = 1 N was used to determine the effect of composite microstructure on its mechanical properties.

The values of $\bar{M}$ and $\bar{H}$ generally increased as porosity, ε, decreased and the composite zircon volume fraction, ϕ_z (zircon volume/total volume), increased (Fig. 2a and b). The maximum temperatures at which the composites were fired are shown in Fig. 2c. It may be observed that, for each value of ϕ, the values of $\bar{M}$ (Fig. 2a), $\bar{H}$ (Fig. 2b), and T (Fig. 2c) aligned in straight lines (which started from ε = 1) except for the points corresponding to ϕ = 0.525 (zircon volume/solids volume) fired at high temperatures (1300 °C and 1350 °C, Fig. 2c) owing to partial zircon solution [9,10] (parallel to increased zircon grain size).

Taking into account that, for a pore-free binary composite, the effect

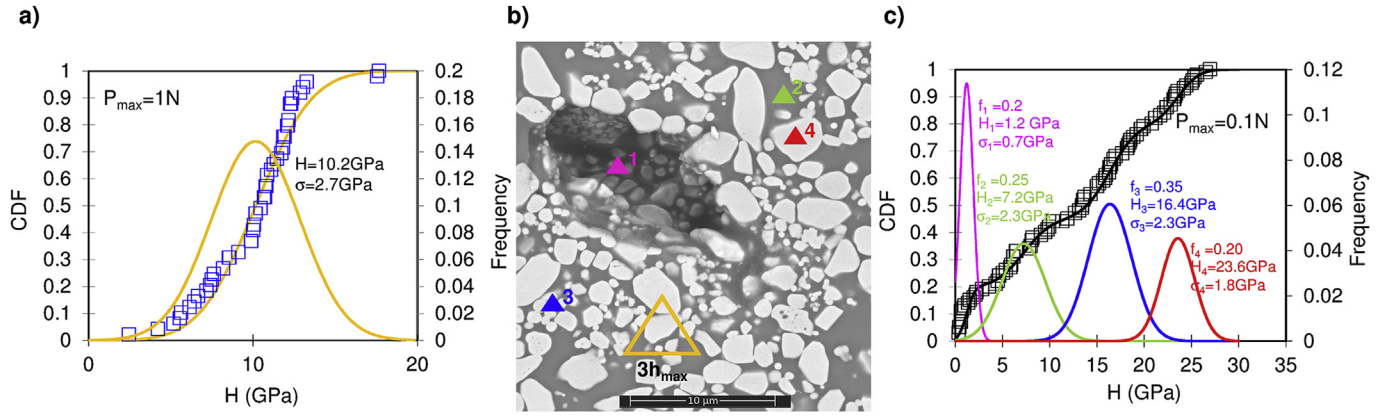

Fig. 1. Cumulative distribution functions (CDFs) and frequency of hardness, H: a) P_{max} = 1 N and c) P_{max} = 0.1 N. The plot in Fig. 1c was deconvoluted into a series of four-mechanical-component CDFs, which were assumed to be Gaussian. b) SEM micrograph of the composite showing the representative volume elements, RVEs, for P_{max} = 1 N (empty yellow triangle) and P_{max} = 0.1 N (solid coloured triangles). Composite ϕ = 0.525 fired at 1350 °C. (For interpretation of the references to colour in this figure legend, the reader is referred to the Web version of this article.)

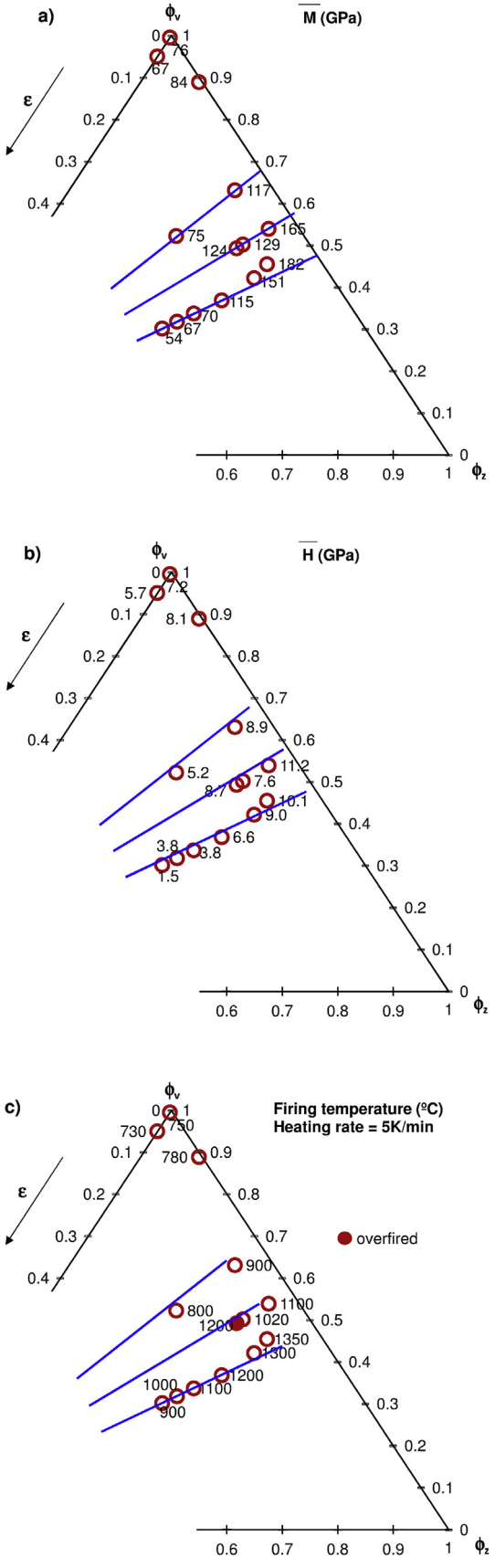

Fig. 2. Effect of porosity, ε, zircon volume fraction, ϕ_z, and glass volume fraction, ϕ_v, on: a) indentation modulus, $\bar{M}$; b) hardness, $\bar{H}$; and c) peak firing temperature.

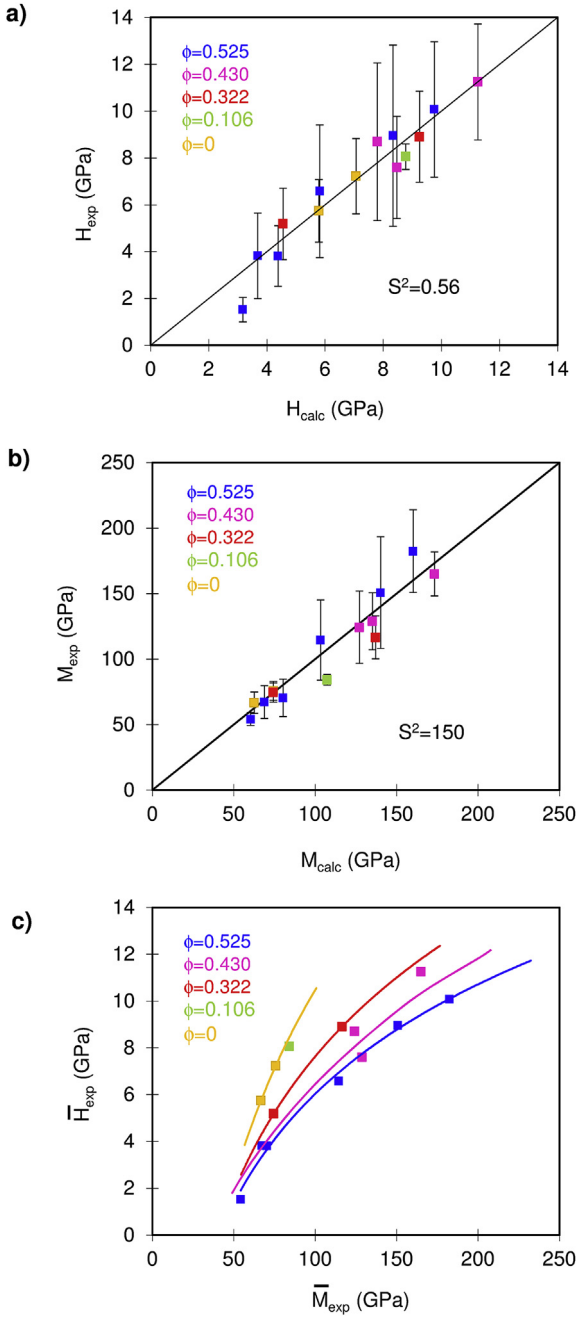

Fig. 3. Fit of the experimental data to the calculated values: a) H from eq. (7) and b) M from eq. (6). c) Relationship between $\bar{M}_{exp}$ and $\bar{H}_{exp}$.

of each component on its mechanical properties follows the mixture rule, one obtains [17,18]:

$$M = [M_g(1 - \phi) + M_z\phi] \quad (4)$$

and

$$H = [H_g(1 - \phi) + H_z\phi] \quad (5)$$

where M_g = 76 ± 7 GPa and H_g = 7.23 ± 1.6 GPa were the experimentally measured glass indentation modulus and hardness; M_z = 397 GPa and H_z = 20.5 GPa were the zircon indentation modulus and hardness, calculated [13] from the values of the elastic modulus and Poisson ratio reported in the literature [19].

Based on the results of Fig. 2, the effect of porosity, ε, on the strain modulus, M, and hardness, H, [17,18], and the effect of grain size, G, on hardness, H, [18], the following equations were proposed to describe

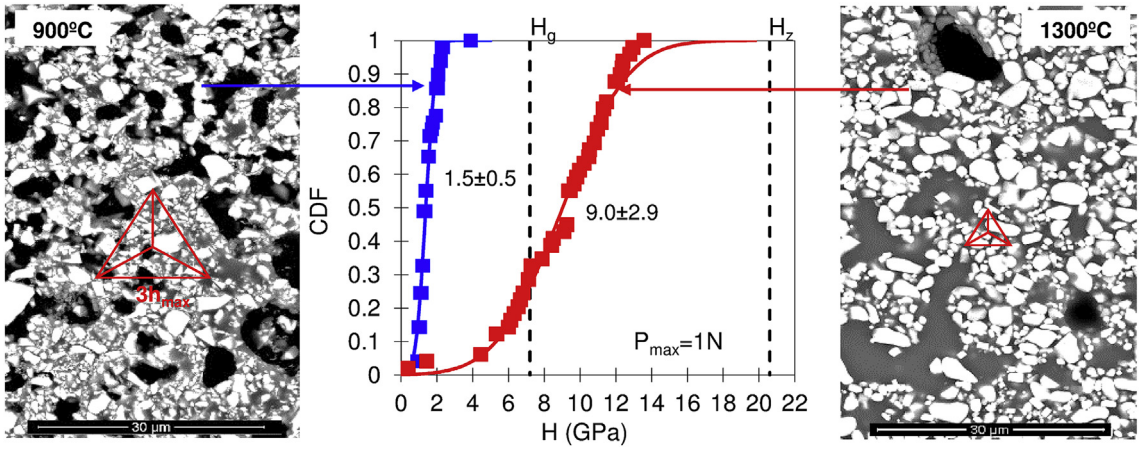

Fig. 4. Cumulative distribution functions, CDFs, of hardness for composite $\phi = 0.525$ fired at 900 °C and 1300 °C. SEM micrograph of these composites showing their corresponding representative volume element, RVE.

the effect of porosity and grain size on H and M:

$$M = [M_g(1-\phi) + M_z\phi]\cdot exp(-a\varepsilon) \quad (6)$$

and

$$H = [H_g(1-\phi) + H_z\phi(1 + bG^{-0.5})]\cdot exp(-c\varepsilon) \quad (7)$$

where a, b, and c are fitting parameters.

The experimentally determined values of H fitted very well to eq. (7) (Fig. 3a) with b = 0.21 $\mu m^{0.5}$ and c = 4.44. The same occurred with M (eq. (6)), a value of a = 3.80 being obtained (Fig. 3b). The values of a and c, which describe how porosity, ε, affected M and H, were similar to those obtained by other researchers [17,18]. On the other hand, it may be observed that the scatter of M and H generally increased as their average value rose (Fig. 3a and b). However, at similar values of $\bar{M}$ and $\bar{H}$, their scatter increased with ϕ. Indeed, for composites with small $\bar{M}$ and $\bar{H}$ (Fig. 4, composite $\phi = 0.525$ at T = 900 °C), the corresponding representative volume element (RVE) was larger than that of its mechanical components (pore, glass, zircon …), so that the experimental values of H and M represented the average mechanical performance of the relatively large RVE area, which therefore varied little from one area to another in the sample (narrow CDF). In contrast, for composites with high $\bar{M}$ and $\bar{H}$ (Fig. 4, composite $\phi = 0.525$ at T = 1300 °C), RVE was of the same order as or smaller than the size of the pores, glass areas, zircon grains, or glass–zircon agglomerates, so that the experimental H and M values varied highly from one indentation to another (wide CDF). In addition, for composites with similar mechanical properties (and hence similar RVEs), the larger the zircon content, ϕ, the greater was generally the heterogeneity of the microstructure [9,10], which also led to greater scatter in the indentation results.

Plotting $\bar{H}_{exp}$ versus $\bar{M}_{exp}$ confirmed that, for each zircon content, ϕ, there was a direct relationship between both (Fig. 3c). Generally speaking, at the same $\bar{H}_{exp}$, the value of $\bar{M}_{exp}$ rose as zircon content, ϕ, increased.

Composites of high hardness (11.3 ± 2.5 GPa) and low porosity ($\rho \approx 0.93$), with a zircon content of $\phi = 0.43$, were obtained at temperatures of about 1100 °C. These results are slightly better than those reported [7] for zircon–glass ceramics composites, also obtained by sintering. It was furthermore verified that the nanomechanical properties of some of these composites were much higher than those obtained in zircon glazes [8]. On the other hand, the relationships obtained in this study (eq. (6) and eq. (7)), which evidence the pronounced influence of porosity and zircon content on the nanomechanical properties of the material, are very useful when it comes to successfully designing ceramic glazes for heavily trafficked floorings.

4. Conclusions

Composites of high hardness (11.3 ± 2.5 GPa) and low porosity ($\rho \approx 0.93$) were obtained at temperatures of about 1100 °C from mixtures with $\phi = 0.43$.

It was verified that the standard deviation of the hardness and modulus of indentation distributions increased with the arithmetic mean of these properties. At similar values of $\bar{M}_{exp}$ and $\bar{H}_{exp}$, scatter increased as composite microstructural heterogeneity grew.

An empirical model was developed that describes the effect of the most important microstructural characteristics (porosity, zircon grain size, and zircon volume/solids volume) of the studied composites on their hardness and modulus of indentation. These relationships are very useful when it comes to designing ceramic coatings (glazes) for heavily trafficked floorings.

Declaration of competing interest

The authors declare that they have no known competing financial interests or personal relationships that could have appeared to influence the work reported in this paper.

Acknowledgements

This study was co-funded by the ERDF Operational Programme for the Valencia Region and the Valencian Institute for Business Competitiveness (IVACE).

References

[1] I.A. Levitskii, S.E. Barantseva, N.V. Mazura, Particulars of structure and phase formation in zirconium-coating frits and glazes, Glass Ceram. 66 (7–8) (2009) 258–261.
[2] A. Bernasconi, V. Diella, N. Marinoni, A. Pavese, F. Francescon, Influence of composition on some industrially relevant properties of traditional sanitary-ware glaze, Ceram. Int. 38 (7) (2012) 5859–5870.
[3] M. Tichell, et al., Study of the development and application of glazes of a glass–-ceramic nature with a view to enhancing the technological properties of conventional glazes, Qualicer 1996. Proceedings of the IVth World Congress on Ceramic Tile Quality. Castellón (Spain), 1996, pp. 201–230.
[4] R. Casasola, J.M. Rincón, M. Romero, Glassceramic glazes for ceramic tiles: a review, J. Mater. Sci. 47 (2012) 553–582.
[5] B. Eftekhari Yekta, P. Alizadeh, L. Rezazadeh, Floor tile glass–ceramic glaze for improvement of glaze surface properties, J. Eur. Ceram. Soc. 26 (16) (2006) 3809–3812.
[6] B. Eftekhari Yekta, P. Alizadeh, L. Rezazadeh, Synthesis of glass–ceramic glazes in the ZnO-Al2O3-SiO2-ZrO2 system, J. Eur. Ceram. Soc. 27 (5) (2007) 2311–2315.
[7] F.M. Bertan, O.R.K. Montedo, C.R. Rambo, D. Hotza, A.P. Novaes de Oliveira, Extruded $ZrSiO_4$ particulate-reinforced LZSA glass–ceramics matrix composite, J. Mater. Process. Technol. 209 (2009) 1134–1142.
[8] K. Pasiut, J. Partyka, M.M. Bucko, M. Grands, L. Kurpaska, W. Piekarczyk, An

impact of the molar ratio of Na_2O/K_2O on nanomechanical properties of glaze materials containing zirconium oxide, J. Alloy. Comp. 815 (2020) 152411.
[9] J.L. Amorós, E. Blasco, A. Moreno, E. Zumaquero, C. Feliu, Non-isothermal sintering of powdered vitrified composites. A kinetic model, Mater. Lett. 236 (2019) 236–239.
[10] J.L. Amorós, A. Moreno, E. Blasco, Viscous flow sintering in glass matrix composites with rigid inclusions, Ceram. Mod. Technol. 3 (2019) 155–162.
[11] W.C. Oliver, G.M. Pharr, An improved technique for determining hardness and elastic-modulus using load and displacement sensing indentation experiments, J. Mater. Res. 7 (1992) 1564–1583.
[12] W.C. Oliver, G.M. Pharr, Measurement of hardness and elastic modulus by instrumented indentation: advances in understanding and refinements to methodology, J. Mater. Res. 19 (2004) 3–20.
[13] A. Deirieh, J.A. Ortega, F.J. Ulm, Y. Abousleiman, Nanochemomechanical assessment of shale: a coupled WDS-indentation analysis, Acta Geotech. 7 (4) (2012) 271–295.
[14] G. Constantinides, K.S. Ravi Chandran, F.J. Ulm, K.J. Van Vliet, Grid indentation analysis of composite microstructure and mechanics: principles and validation, Mater. Sci. Eng. A 430 (2006) 189–202.
[15] J.J. Roa, E. Jiménez-Piqué, J.M. Tarragó, M. Zivcec, C. Broeckmann, L. Llanes, Berkovich nanoindentation and deformation mechanisms in a hard metal binder-like cobalt alloy, Mater. Sci. Eng. A 621 (2015) 128–132.
[16] G.M. Pharr, E.G. Herbert, Y. Gao, The indentation size effect: a critical examination of experimental observations and mechanistic interpretations, Annu. Rev. Mater. Res. 40 (2010) 271–292.
[17] F.J. Paneto, J.L. Pereira, J.O. Lima, E.J. Jesus, L.A. Silva, E. Sousa Lima, et al., "Effect of porosity on hardness of Al_2O_3–$Y_3Al_5O_{12}$ ceramic composite", Int. J. Refract. Metals Hard Mater. 48 (2015) 365–368.
[18] Z. Negahdari, M. Willert-Porada, C. Pfeiffer, Mechanical properties of dense to porous alumina/lanthanum hexaaluminate composite ceramics, Mater. Sci. Eng. A 527 (2010) 3005–3009.
[19] T. Beirau, W.D. Nix, U. Bismayer, L.A. Boatner, S.G. Isaacson, R.C. Ewing, Anisotropic mechanical properties of zircon and the effect of radiation damage, Phys. Chem. Miner. 43 (9) (2016) 627–638.